Statistical analysis of rockfall volume distributions: Implications for rockfall dynamics

Carine Dussauge
Laboratoire Interdisciplinaire de Géologie et de Mécanique, Université Joseph Fourier, Grenoble, France

Jean-Robert Grasso[1] and Agnès Helmstetter[1]
Laboratoire de Géophysique Interne et Tectonophysique, Observatoire de Grenoble, Université Joseph Fourier, France

Received 25 May 2001; revised 20 December 2002; accepted 11 February 2003; published 3 June 2003.

[1] We analyze the volume distribution of natural rockfalls on different geological settings (i.e., calcareous cliffs in the French Alps, Grenoble area, and granite Yosemite cliffs, California Sierra) and different volume ranges (i.e., regional and worldwide catalogs). Contrary to previous studies that included several types of landslides, we restrict our analysis to rockfall sources which originated on subvertical cliffs. For the three data sets, we find that the rockfall volumes follow a power law distribution with a similar exponent value, within error bars. This power law distribution was also proposed for rockfall volumes that occurred along road cuts. All these results argue for a recurrent power law distribution of rockfall volumes on subvertical cliffs, for a large range of rockfall sizes (10^2–10^{10} m^3), regardless of the geological settings and of the preexisting geometry of fracture patterns that are drastically different on the three studied areas. The power law distribution for rockfall volumes could emerge from two types of processes. First, the observed power law distribution of rockfall volumes is similar to the one reported for both fragmentation experiments and fragmentation models. This argues for the geometry of rock mass fragment sizes to possibly control the rockfall volumes. This way neither cascade nor avalanche processes would influence the rockfall volume distribution. Second, without any requirement of scale-invariant quenched heterogeneity patterns, the rock mass dynamics can arise from avalanche processes driven by fluctuations of the rock mass properties, e.g., cohesion or friction angle. This model may also explain the power law distribution reported for landslides involving unconsolidated materials. We find that the exponent values of rockfall volume on subvertical cliffs, 0.5 ± 0.2, is significantly smaller than the 1.2 ± 0.3 value reported for mixed landslide types. This change of exponents can be driven by the material strength, which controls the in situ topographic slope values, as simulated in numerical models of landslides [*Densmore et al.*, 1998; *Champel et al.*, 2002]. *INDEX TERMS:* 5104 Physical Properties of Rocks: Fracture and flow; 1815 Hydrology: Erosion and sedimentation; 8122 Tectonophysics: Dynamics, gravity and tectonics; *KEYWORDS:* rockfalls, landslides, natural hazard, power law distribution, fragmentation, self-organized criticality

Citation: Dussauge, C., J.-R. Grasso, and A. Helmstetter, Statistical analysis of rockfall volume distributions: Implications for rockfall dynamics, *J. Geophys. Res.*, *108*(B6), 2286, doi:10.1029/2001JB000650, 2003.

1. Introduction

[2] Rockfalls, rockslides, and rock avalanches are defined as rapid movements of rocks driven by global gravity forces, having their origin on steep rock slopes, including subvertical cliffs. These phenomena are a subset of the more general landslide phenomena, which can include falls, slumps, and slides in all kind of ground material from stiff rock mass to unconsolidated or poorly cemented materials [*Varnes*, 1978; *Keefer*, 1999]. The word rockfall is usually used to describe small phenomena, ranging in size from block falls of a few dm^3 up to 10^4 m^3 events. Rockslides sometimes involve more than 10^5 m^3, and rock avalanches can reach several million cubic meters [*Varnes*, 1978; *Keefer*, 1984, 1999]. In this study we will use the rockfall label without any volume distinction, nor distinction in the failure mechanism.

[3] As for floods, earthquakes or volcanic eruptions, evaluating rockfall dynamics means analyzing the location, size, and time patterns of rockfall events. Here we focus on the distribution of rockfall volumes. For some natural

[1]Now at Institute of Geophysics and Planetary Physics, University of California, Los Angeles, California, USA.

0148-0227/03/2001JB000650$09.00

phenomena, including floods and earthquakes, statistical analysis are used to derive the recurrence rate of an event of a given size. The flood sizes are proposed to follow an exponential distribution [e.g., *Guillot and Duband*, 1967; *U.S. Water Resources Council*, 1982], whereas the earthquake sizes are best fitted by a power law distribution [*Gutenberg and Richter*, 1949]. On the first hand, the size distribution can be used for hazard assessment, if we hypothesize the distribution to be stationary over time. On the other hand, the type of distribution can provide routes to further investigate the underlying physical processes.

[4] Power law distributions have been suggested to characterize rockfall distributions triggered along road cuts [*Noever*, 1993; *Hungr et al.*, 1999], or natural cliffs [*Gardner*, 1970; *Wieczorek et al.*, 1995]. In this study we analyze the volume distributions of rockfalls from natural cliffs, in different geological settings, different volume ranges and different timescales. Contrary to earthquakes, rainfalls, or floods, few if any natural slopes or cliffs are continuously monitored in order to provide the exact time of occurrence, location, and size of rockfall events. Because of the lack of instrumental monitoring of rockfalls, the available inventories are weak compared to some other natural phenomena, with several possible biases induced by non homogeneous sampling in time, space and size domains. We test how reports of rockfall activity can be used to investigate rockfall volume distribution, the way other scientists used historical catalogs to further constrain contemporary, short time, instrumental catalogs [e.g., *Wesnousky et al.*, 1983, 1984].

[5] We compare volume distributions of natural rockfalls that occurred on Grenoble cliffs, French Alps [*Service de Restauration des Terrains de Montagnes de l'Isére* (*RTM*), 1996], Yosemite cliffs, Sierra Nevada, California [*Wieczorek et al.*, 1992] and a worldwide inventory of large rockslides [*Couture*, 1998]. The first two case studies investigate the same temporal scale, about one century, and the same spatial scale, roughly 100 km of cliff length. The main difference between these two case studies is the involved rock masses, layered calcareous cliffs and massive granite rock cliffs, for Grenoble and Yosemite catalogs respectively. For each area, we validate statistically the power law distribution function as an estimate for the observed rockfall volume distribution. Exponent values are similar, within error bars, for the three data sets. This suggests that the distribution law for rockfall volume does not depend on either the geological setting or the scale of observation. These results are similar to analysis of rockfalls that occurred along road cuts [*Noever*, 1993; *Hungr et al.*, 1999]. We show how this distribution law can be used for rockfall hazard assessment, by analyzing the validity domains and limits of this approach. We investigate the possible mechanical models that can reproduce this power law distribution of rockfall volumes.

2. Data

2.1. The Grenoble Rockfall Inventory, French Alps

[6] The first data set reports rockfall volume that occurred on subvertical cliffs surrounding the urban area of Grenoble city, French Alps [*RTM*, 1996]. In order to characterize the geological setting of the cliff, we need to identify the forces acting on this system. Such forces are the long-term tectonic forces due to plate tectonic dynamics. Intermediate-term and short-term forces that act on the cliffs are climatic forcing (i.e., glacial unloading, fluvial incision, temperature, rain, snow, and winds) and earthquake waves, as sorting by increasing time frequency of applied forces. To cast the cliff geological settings, the rate of base level fall (which can be due to any combination of differential rock uplift rate between cliff and valley and fluvial or glacial incision), is the more relevant parameter to characterize the hillslope. Because this parameter is not estimated for the cliff we studied, we use a local differential displacement or a local deformation rate as a proxy to characterize the cliff deformation rate.

[7] These Grenoble cliffs are part of the Chartreuse and Vercors subalpine massifs, made of sedimentary rocks from upper Jurassic and lower Cretaceous age (limestone and marls). Initial bedding is folded and faulted due to alpine horizontal compressive stresses, resulting mostly in subvertical fractures across gently inward dipping stratification (Figure 1). The cliffs dimensions are 50 m to 400 m in height, 120 km in length, as cumulative values on two successive rocky walls (Figure 1). The cliffs elevation ranges from 800 m to 2000 m. For such an altitude, in the French Alps, the climatic conditions correspond to wet springs and falls seasons and frozen conditions in wintertime. The Chartreuse-Vercors massif is suggested to have a weak local deformation rate, i.e., less than a few mm/yr either for horizontal or for vertical displacements [*Martinod et al.*, 1996]. These values are differential displacement we used as a proxy of cliff deformation rates. They come from GPS surveys on Chartreuse Vercors sites. The benchmarks are located 10-20 km apart from each others all above the cliff edges that extend over 70 km in length in the Grenoble area [*Martinod et al.*, 1996]. Historical and instrumental seismicity rates are low, with a few $M = 4$ earthquakes reported in the area during the last 5 centuries [*Fréchet*, 1978; *Grasso et al.*, 1992]. There is no report on rockfalls possibly triggered by earthquakes. One possible change in loading conditions is the last glacial unloading (Würm, dated 10^4 years before present). Unloading the cliff faces from the ice pressure induces a viscoelastic rebound of the cliffs. The phenomenon is mechanically not well quantified on the cliffs because of the difficulty to evaluate the long-term rheology of the cliff.

[8] Rockfall activity that occurred in the Grenoble calcareous Alps from 1248 to 1995 was reported by the Restauration des Terrains de Montagnes office (RTM), a forestry office in charge of natural risks in the French Alps, since 1870 [*RTM*, 1996]. As the RTM office was created in 1870, the 1870–1890 period is the threshold between archive reports for rockfall events and the specific survey of mountain slopes. For each event the available data from the Grenoble catalog are (1) the location of the rockfall, (2) the date of occurrence, and (3) the volume and the induced damages. Most of this information has been reported by forest guards as described in section 1, with a sampling rate of once every a few weeks. For some roughly estimated volumes, we provide new volume estimates on the basis of in situ observation and reanalysis of reports. Reported volumes range from 3×10^{-2} m^3, i.e., typical of a slight damage on a single house, to 5×10^8 m^3. The largest event

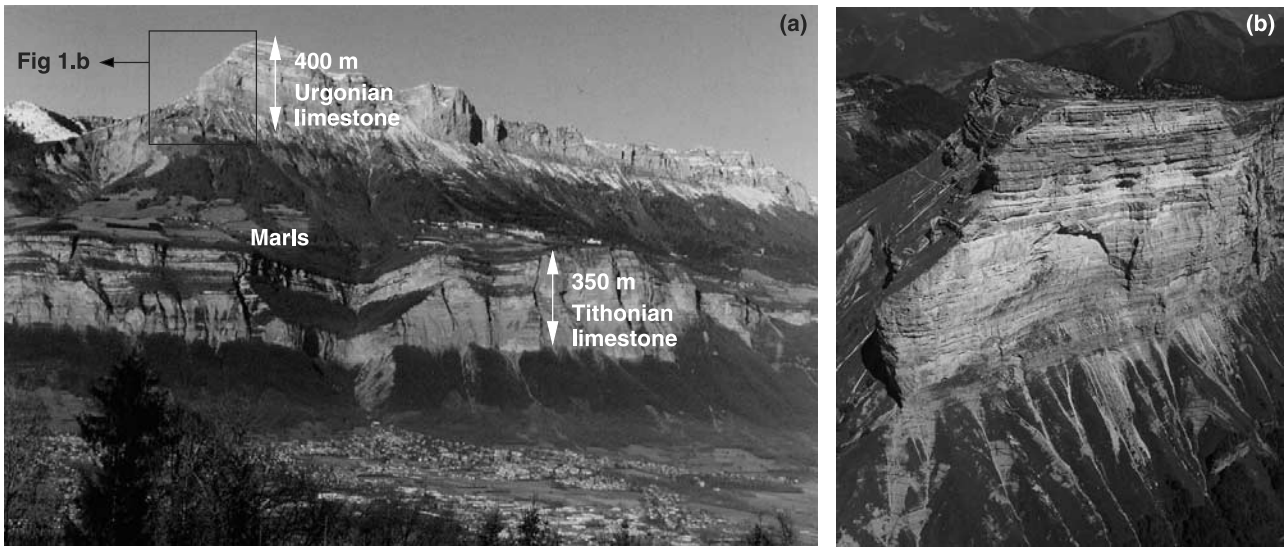

Figure 1. East face of the Chartreuse massif, Grenoble, France. (a) Subvertical calcareous cliffs are separated into two levels; the intermediate, less steep, slope is associated with marly levels. The maximum height of each level is 350–400 m, and the total length of cliffs is 120 km. Note the suburban area of Grenoble at the bottom of the cliffs. The photograph, by J. M. Vengeon, is roughly 5% of the total area covered by the Grenoble rockfall inventory [*RTM*, 1996]. (b) Geometry of the fracture pattern, as detailed from top of the cliff in Figure 1a. It is roughly characterized by subhorizontal bedding and subvertical orthogonal joints; the small vertical joints are not visible at the scale of Figure 1b.

of this data set is the 1248 Mount Granier rock avalanche, 40 km north of Grenoble, with a volume of 5×10^8 m^3 [*Goguel and Pachoud*, 1972].

[9] For this data set, threshold values are estimated by RTM forest guards. They report they never missed a 500 m^3 event size, because of its impact on either infrastructures or on forest structures involving forests, meadows, trails, roads, housing (RTM, personal communication, 2000). Such large events induce changes in the cliff pattern (scars, change in color, geometry) as well. Alternatively, forest guards report they missed a large number of small events, which are to small to induce a significant and visible damage. Up to events close to 10 m^3, they report they can miss events. We thus assume the Grenoble inventory to be complete for volumes greater than 500 m^3. Because of the nonuniform temporal sampling (Figure 2), one large event in 1248 and just a few ones reported in the 17th–19th centuries period, we select events within the 1935–1995 time window only. This period is a trade-off between a minimum number of available events and a period for which the sampling can be considered as uniform. On such a basis, the Grenoble catalog we used involves 87 events.

2.2. The Yosemite Valley Rockfall Inventory, California

[10] The second data set gathers rockfalls that occurred in the Yosemite Valley, Sierra Nevada, California [*Wieczorek et al.*, 1992]. It concerns cliffs of massive granite from Cretaceous age. The total area covers almost 100 km of cliff length. Cliffs have a maximum height of 1000 m, with a mean value of 300 m, and an elevation ranging from 1000 to 2300 m (Figure 3). The climatic setting is roughly a dry and warm spring and summer and cold wet falls and winter. Rockfalls result partly from exfoliation and sheeting processes that are induced by the release of pressure of previously buried rocks (Figure 3). The resulting sheets tend to be mainly parallel to the topography [*Huber*, 1987].

[11] This area is part of the Sierra Nevada "block" which is moving with respect to the stable North American plate. Local differential displacement rates deduced from a GPS survey of less than a millimeter per year if any, is related to San Andreas tectonics plus shear strain associated with Owens Valley and associated faults [*Dixon et al.*, 2000]. The U.S. Sierra uplift rate is less than a millimeter per year, the uplift rate being not resolved by a 5 years GPS survey [*Dixon et al.*, 2000]. Only about 5% of the rockfalls are reported as triggered by earthquakes [*Wieczorek et al.*, 1992]. Last glacial unloading corresponds to the end of the Tioga epoch, 15000 years BP at relatively low elevation [*Huber*, 1987].

[12] The historical Yosemite rockfall inventory reports 395 events in the 1850–1992 period [*Wieczorek et al.*, 1992]. Most of them are reported by either National Park Rangers or USGS geologists. As for the Grenoble inventory, there are large uncertainties on reported volumes, and a nonuniform sampling of small volume rockfalls over time. The sampling rate is globally shorter than one month, observed data being collected in the Superintendent Monthly report. This sampling rate has been much shorter in the last ten years (G. F. Wieczorek, personal communication, 2000). The threshold for the inventory completeness for the small events is not estimated.

[13] There are two classes of volume estimates in the Yosemite inventory. For one class of rockfalls, roughly one quarter of the inventory, the reports allow a quantitative estimate of volumes. For the second class, only qualitative estimates are given. Following the same criterion as for the Grenoble catalog, we select events with quantitative volume

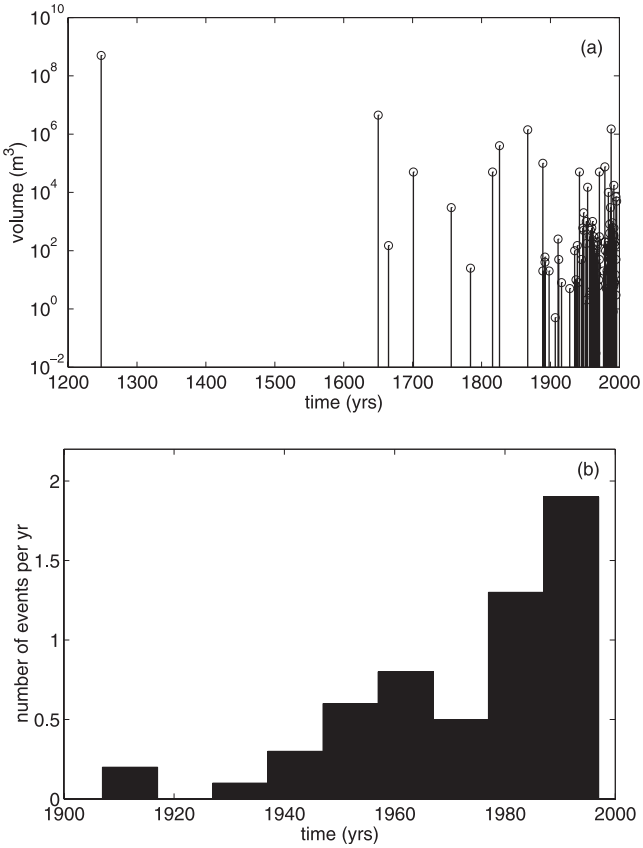

Figure 2. Occurrence rate for rockfalls for Grenoble area, RTM (1996) inventory. (a) Volumes and time of occurrence in the 1200–1995 period. (b) Occurrence rate in the 1935–1995 period for volume larger than 50 m^3. Because of the nonuniform temporal and volume samplings, the studied catalog is restricted to the 1935–1995 period, involving 87 events with volumes ranging from 10^{-2} to 10^6 m^3.

estimates in the 1915–1992 period (Figure 4). We obtain 101 events, with volumes ranging from 1 to 6×10^5 m^3. Because qualitative volume estimates exist in the inventory for volumes as large as a few thousands cubic meters, this volume catalog is not complete up to large volumes. We will consider this volume inventory as a subset of the genuine volumes of the Yosemite rockfall population, for the 1915–1992 period.

2.3. A Worldwide Rockfall Inventory

[14] The last data set we use is a worldwide collection of large rockslides and rock avalanches, as old as the last glacial epoch [*Couture*, 1998]. Contrary to the two previous data sets of rockfalls that occurred within homogeneous geological setting, e.g., calcareous and granite cliffs, respectively, *Couture* [1998] gives an overview of the phenomenology of rock avalanches on Earth and other planets. Therefore the geological setting of these events is obviously heterogeneous, and the sampling method just comes out from a bibliographic study.

[15] From the Couture inventory, we selected 142 Earth events. Estimated volumes are provided by historical reports, based on observations of cliff scars and deposits or on geomorphological patterns for the oldest events. The collection is not supposed to be exhaustive [*Couture*, 1998]. The sampling is neither uniform in time, recent events being more often reported than older ones, nor in space domain. Also, the sampling is not uniform in size, the largest events being preferentially reported in historical reports. Like the Yosemite inventory, this data set is one subset of the complete worldwide catalog.

2.4. Measurement Techniques for Rockfall Inventories

[16] Concerning the study of earthquakes, rainfalls or floods, instrumental monitoring provides direct or indirect estimates of events occurrence in size, time, and space domains. Few instrumental measurements exist for the study of the rockfall activity, especially concerning natural cliffs. One study uses a continuous seismic monitoring to detect rockfall events and to size up rockfall volumes on a single, well-defined cliff [*Rousseau*, 1999]. *Rousseau* [1999] uses a seismic model to derive the volume of a rockfall event from the amplitude of the recorded seismic signals. Generally, data about rockfalls are mainly reported by forest guards or road surveyors without the help of any quantifying tool.

[17] Because of this lack of instrumental monitoring, the rockfall volume inventories we used suffer several possible biases. First, the sampling in time domain is driven by the visit rate of the field survey observer, this survey being usually part of a forestry or road survey (not specific to rockfall observation). For some events, the field evidences can disappear within the laps time of two visits. For other events, the visit rate can induce a cumulative effect on rockfall volumes estimates, i.e., all the rockfalls which occurred at the same place are estimated as one single event at the sampling rate resolution.

[18] Second, in size domain, rockfall events are reported mainly when they induce damages to natural or anthropic entities. Impacts on forest trees, trails, roads, and housing are the main criteria to report the occurrence of a rockfall event. Therefore the rockfalls which did not induce damages are seldom reported. This induces a censoring effect for the so-called small events. Small volumes are also under sampled because of the screening effect due to man-made protective structures, such as rock fences or forests. As a consequence, noninstrumental inventories are obviously incomplete for the small events.

[19] Another possible bias emerges from the inaccuracy of volume estimates, which are based on the observation of the volume of deposits, sometimes coupled with the observation of the visible scar on the slope. Error bars for volumes are thus large and difficult to quantify. For large rockfall volumes, i.e., volumes greater than a few hundreds of cubic meters, the volume estimate comes from the area covered with new rock material and its thickness values along the slope. For smaller rockfalls the sum of the volumes of the largest blocks is usually used as a volume estimate. When visible, the surface of the cliff scar that is induced by the rockfall is further used, its thickness being more difficult to assess.

3. Statistical Analysis of Volume Distribution

[20] For the three data sets, we test which distribution function best describes the rockfall volume data. For each

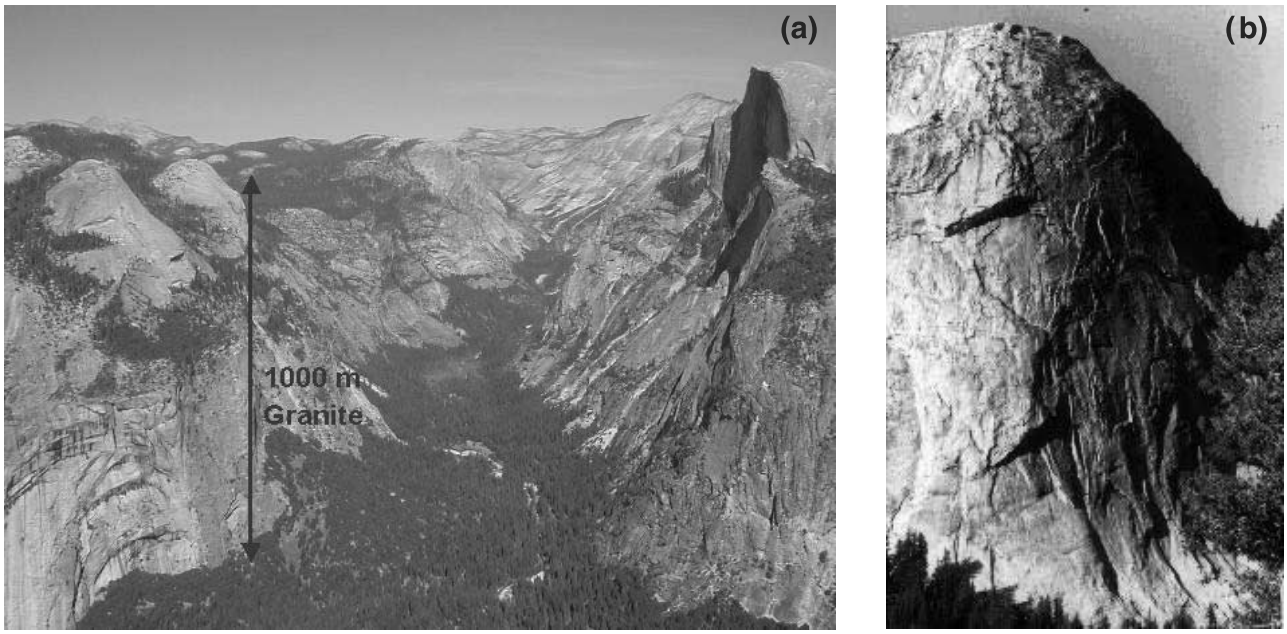

Figure 3. Cliffs surrounding the Yosemite Valley, California Sierra. (a) Subvertical granitic cliffs, maximum height 800–1000 m, total length 100 km; photograph by G. Wieczorek. (b) Detailed view of the Fairview dome. The fracture pattern is roughly characterized by a sheeting process giving joints parallel to the topography, and spaced subvertical joints; photograph by J. R. Grasso.

catalog, the selected events correspond to the time window for which the catalog is supposed to be homogeneous in the time domain. Because of the censoring effect, there is an under sampling of small volume events. For the largest observed volumes, with a size comparable to the cliff height, the distribution may be truncated because of finite size effects. Accordingly, we select only rockfall events above a given volume. This minimum volume is a priori unknown and will be estimated from the adjustment of distribution laws to the data. First we search which distribution functions may describe our data. Second, using the χ^2 criterion, we test if the rockfall volume distribution is consistent with the hypothesized distribution functions.

3.1. Grenoble Inventory

[21] The observed cumulative distribution for the Grenoble cliffs is evaluated for the 87 rockfall events in the 1935–1995 period (Figure 5). The distribution is almost linear in a log-log plot for volumes larger than 40 m^3. For volumes smaller than 40 m^3, we observe a downward departure from the linear behavior that is typical of a censoring effect. Accordingly, we test how the observed cumulative volume distribution may be adjusted by a power law distribution for the 55 events of volume above 40 m^3, i.e.,

$$N(V) \sim V^{-b}, \tag{1}$$

with V the rockfall volume, $N(V)$ the number of events greater than V and b a constant parameter. To estimate the exponent value, b value, we used the maximum likelihood and linear regression methods because there are the two methods classically suggested in the literature [e.g., *Pickering et al.*, 1995]. Maximum likelihood and linear regression estimates are not independent estimates.

[22] Following *Aki* [1965], the maximum likelihood estimate for b is

$$b = \frac{1}{\ln(10)(\langle \log(V) \rangle - \log(V_0))}, \tag{2}$$

in the case of a pure power law distribution, with a standard deviation determined by

$$\sigma = \frac{b}{\sqrt{N_0}}, \tag{3}$$

where V_0 is the minimum volume used in the power law fit, $\langle \log(V) \rangle$ is the average of $\log(V)$ for events larger than V_0 and N_0 the number of events with volume larger than V_0. A more complex equation is necessary when the distribution is bounded to a given V_{max} value. This is not the case of the data we fit, i.e., we have no a priori bound on the maximum volume size.

[23] For the Grenoble inventory, these two techniques provide similar values, $b \sim 0.40$ (Table 1). The standard deviation of b given by equation (3) is 0.06, as estimated from the maximum likelihood method. These values are not sensitive to either a V_0 value increase above 40 m^3 or a change in the analyzed time period. Second, we use the χ^2 test to validate the hypothesis that the observed volume distribution follows a power law distribution for volumes larger than 40 m^3. The χ^2 test compares an observed histogram to a histogram obtained by sampling the hypothesized distribution function [e.g., *Press et al.*, 1992; *Taylor*, 1997]. The χ^2 value measures a distance between these two histograms, as defined by

$$\chi^2 = \sum_{i=1}^{k} \frac{(n_i - n_i^*)^2}{n_i^*}, \tag{4}$$

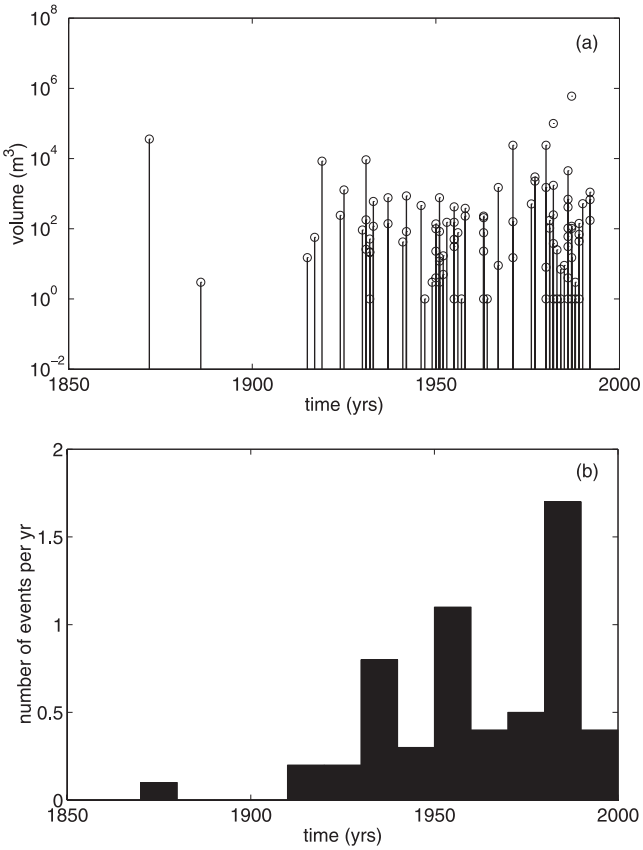

Figure 4. Occurrence rate for rockfalls from the Yosemite Valley data set [*Wieczorek et al.*, 1992]. (a) Volume and occurrence for the 1850–1992 period. (b) Occurrence rate in the 1850–1992 period for volume larger than 50 m^3. Because of the nonuniform temporal sampling shown on the 1850–1992 period, the time window selected for the study is 1850–1995, involving 101 events with volumes ranging from 1 to 10^6 m^3.

where n_i is the observed number of events in the ith bin, and n_i^* is the expected number for the hypothesized distribution function. Equation (4) follows a so-called χ^2 probability law, that allows evaluating the probability to overpass the χ^2 value when the tested hypothesis is true. We use the reduced χ^2_r value [*Press et al.*, 1992; *Taylor*, 1997], obtained by dividing the χ^2 value by the number of degrees of freedom of the system, n_f defined by

$$n_f = (\text{number of bins}) - c, \tag{5}$$

where c is the number of constraints applied for the χ^2 test. For our application, $c = 2$, with one constraint for the parameter of the law in the case of the power law, and one for the binning of the data in equiprobable classes [*Press et al.*, 1992; *Taylor*, 1997]. A reduced $\chi^2 \gg 1$ rejects the tested distribution as a possible description of the data.

[24] Because the χ^2 test requires Gaussian-distributed numbers of objects per bin, we have a trade-off between the appropriate number of bins and the number of objects within each class. Using 11 bins, corresponding to 5 events per bin, we obtain a reduced χ^2 value of 0.58. The power law distribution is thus accepted by the test with a 95% confidence value. We have tested different values of bin numbers between 5 and 18. The reduced χ^2 value is always close to 1, so that the power law distribution is always accepted at the 95% confidence level. With the same type of analysis, we reject other distribution functions, such as the exponential, Weillbull and Gumbel distributions, to fit the Grenoble rockfall volume distribution in the same volume range.

3.2. Yosemite Inventory

[25] The rockfall volume distribution from the Yosemite inventory is built with 101 events that occurred in the

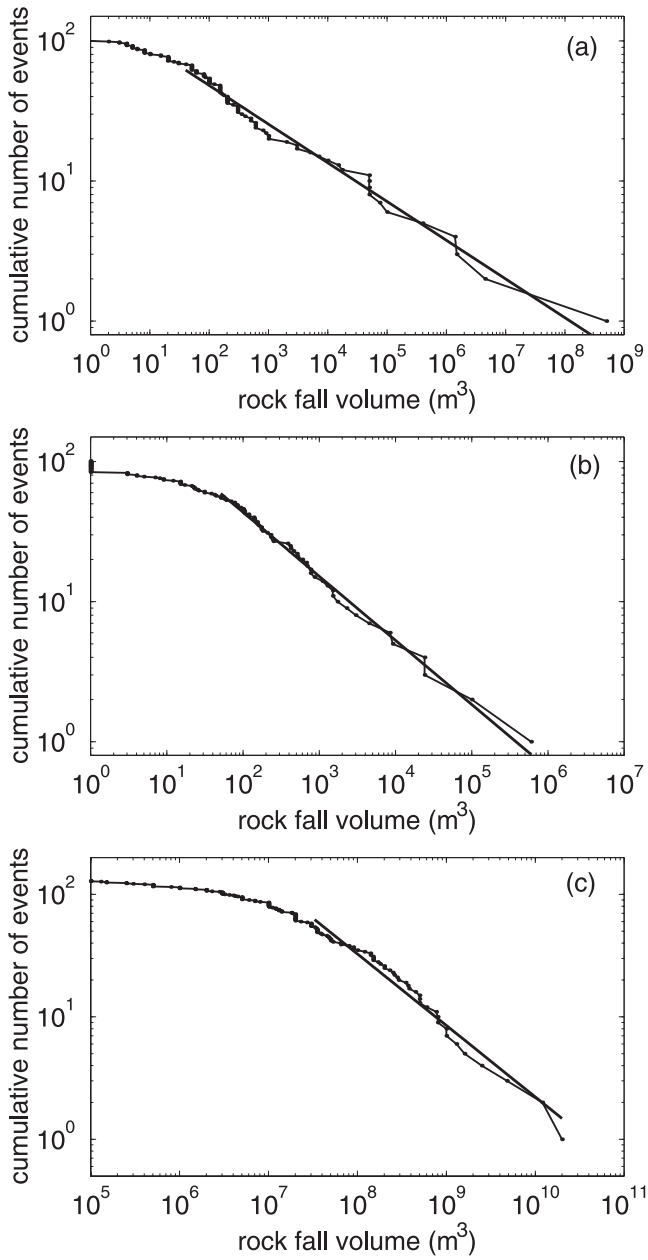

Figure 5. Cumulative volume distributions for rockfalls. For each plot, the straight line is a fit by a power law for volumes larger than V_0, estimated by linear regression. The exponent values and the χ^2_r values are given in Table 1; see text for details. (a) Grenoble area; (b) Yosemite Valley; (c) worldwide inventory.

Table 1. Characteristics of Rockfall Volume Distributions for the Three Studied Data Sets[a]

Site	Time Window	N_{events}	V_{obs}, m^3	V_0, m^3	N_{fit}	b_{lr}	b_{ml}	χ_r^2
Grenoble, France	1935–1995	87	10^{-2}–10^6	40	55	0.40	0.41 ± 0.06	0.58
Yosemite, USA	1915–1992	101	1–10^6	50	56	0.46	0.45 ± 0.06	0.72
Worldwide	10,000 years	142	10^3–2×10^{10}	3.1×10^7	54	0.58	0.51 ± 0.07	1.07

[a] b_{lr} is the linear regression estimate of b value; b_{ml}, the maximum likelihood estimate of b value; V_{obs}, the range of observed volume values; V_0, the value of minimum volume used for power law fit; χ_r^2, the reduced χ^2 value.

1915–1992 period (Figure 5). As for the Grenoble data set, we recover (1) a roughly linear pattern on a log-log plot for volumes larger 50 m^3 and (2) a downward departure from the linear pattern for small volumes. For the 56 events of volume above 50 m^3, we obtain $b = 0.45$ from the maximum likelihood with a standard deviation of 0.06. Using the linear regression method we recover a similar b value (Table 1). The b value is not sensitive to changes in either the time period or the minimum volume above 50 m^3.

[26] Using 11 bins, corresponding to 5 events per bin, we obtain a reduced χ^2 value of 0.72. Therefore the hypothesis that the rockfall volumes follow a power law is accepted at the 90% confidence level.

3.3. Worldwide Inventory

[27] The 142 events of the worldwide inventory range in size from 10^4 to 10^{10} m^3. The cumulative volume distribution shown in Figure 5 mimics the two previously analyzed data sets. For the 54 events with a volume greater than 3×10^7 m^3, the observed distribution is well fitted by a power law distribution with $b = 0.51$, in agreement with the other data sets (Table 1). Using 10 bins, corresponding to 5 events per bin, we obtain a reduced χ^2 value of 1.07. Therefore the hypothesis that the rockfall volumes follow a power law distribution above 10^7 m^3 is accepted at the 90% confidence level. Similar results are obtained when testing different bin numbers between 5 and 10.

4. Discussion

4.1. Synthesis of Observed Rockfall Volume Distributions

[28] The three originally analyzed data sets display power law distributions of rockfall volumes, with similar power law exponents, i.e., in the range 0.4–0.6 ± 0.06. The Yosemite and Grenoble cliffs are both steep cliffs made of strong rock, with the same cliff length. The geometries of the discontinuity patterns are different for the two cliffs. Subvertical fractures across gently dipping stratification characterize the Grenoble sedimentary cliffs, while exfoliation and sheeting of granitic domes are reported for Yosemite cliffs. This suggests that the geometry of the fracturing pattern does not influence the exponent of the power law distribution of rockfall volumes.

[29] When taking together the three catalogs studied here and the other results for rockfalls on subvertical cliffs, including natural rock slopes and road cuts (Table 2), it suggests that rockfall volume distributions follow a power law distribution, with an average exponent of 0.5 ± 0.2 on a 10^{-3} m^3 to 10^{10} m^3 volume range. For the data sets listed on Table 2, even the largest events fit the power law distribution, without any cutoff. No finite size effect is thus observable. However, a possible finite size effect would come from the finite geometry of the rock slopes or cliffs. In particular, the height of cliff is a saturation length for the maximum available rockfall volumes on any given site.

[30] Except for the seismically instrumented cliff on the Reunion island [*Rousseau*, 1999], all the reported rockfall volumes come from field evaluation (Table 2). As events are reported mainly when they induce damage to man-built or natural structures, the sampling is not uniform in the size domain. This sampling bias results in an underestimation of the number of small events. This bias is the best candidate to account for the recurrently observed deficit of small events relatively to the power law distribution for large volumes (Figure 5). There is no evidence that this bias may induce spurious power law behavior. However, it may lead to underestimate the exponent of the power law (e.g., see *Stark and Hovius* [2001] for tests on landslides).

Table 2. Characteristics of Rockfall Volume Distributions on Subvertical Cliffs

Site	Geological Setting	Duration	N	V_{obs}, m^3	V_0, m^3	b[a]	Ref[b]
Grenoble, French Alps	calcareous cliffs	1935–1995	87	10^{-2}–10^6	40	0.41	6(1)
Yosemite, California	granitic cliffs	1915–1992	101	1–10^6	50	0.45	6(2)
Worldwide	undifferentiated cliffs	10,000 years	142	$10^3 - 2 \times 10^{10}$	3×10^7	0.51	6(3)
Reunion Island, Indian Ocean	basaltic cliffs	May–Aug. 1998	370	$\leq 9 \times 10^6$	10^3–10^{5c1}	0.5[c]–1[c]	1, 5
Himalaya, India	road cuts	...	200	10^{-6}–10^6	10	0.19	4
Himalaya, India	road cuts	...	200	10^{-2}–10^7	10	0.23	4
Alberta, Canada	calcareous and quartzitic cliffs	two summers	409	10^{-6}–10	10^{-2}	0.72	2
British Columbia, Canada	massive felsic rock, road cuts[c1]	30 years	389	10^{-2}–10^7	10^{-2}	0.43	3[d1]
British Columbia, Canada	massive felsic rock, road cuts	13 years	123	10^{-2}–10^7	1	0.40	3[d2]
British Columbia, Canada	jointed metamorphic, rock, road cuts[d3]	...	64	10^{-2}–10^7	1	0.70	3[d3]
British Columbia, Canada	jointed metamorphic, rock, road cuts[d4]	22 years	122	10^{-2}–10^7	1	0.65	3[d4]

[a] Exponent for cumulative volume distribution.

[b] References are 1, K. Aki (personal communication, 2002); 2, *Gardner* [1970]; 3, *Hungr et al.* [1999]; 4, *Noever* [1993]; 5, *Rousseau* [1999]; 6, this study, data from (1) *RTM* [1996]; (2) *Wieczorek et al.* [1992]; and (3) *Couture* [1998].

[c] Exponent deduced from amplitude of seismic signals using different models, see text for details: c1, accordingly, the absolute volumes are dependent of the exponent values for each of the seismic model.

[d] Studies on different locations in the same area: d1, Highway 99, bands A and B; d2, BCR; d3, Highway 1; d4, CP.

Table 3. Characteristics of Volume Distributions for Mixed Landslide Types[a]

Site	Geological Setting	N	V, m^3	b	Ref[b]
Southern Alps,	35° mean slope	4984	10^6–3×10^7	0.8	4
New Zealand, Japan,		650	3×10^4–3×10^7	0.66	4
Akaishi Mountains, Japan	nonvertical slope	3243	10^4–10^6	0.64	4, 8
Akaishi Mountains, Japan	nonvertical slope	3243	10^4–10^6	1.25[c]	5, 7, 8
Challana Valley, Bolivian Andes	nonvertical slope	1130		1.07[c]	5, 7, 1
Challana Valley, Bolivian Andes	nonvertical slope	1130		1.25[c]	5, 1
Northridge, California, earthquake triggered	unconsidated earth and debris materials	11,000		0.86[c]	5, 3
Northridge, California, earthquake triggered	unconsidated earth and debris materials	11,000		1.07[c]	7, 3
Eden Canyon	10-35° slope uncons.	709		1.4[c]	5, 6
USA	materials				

[a]All the exponent values are for the cumulative volume distributions.

[b]References are 1, *Blodgett et al.* [1996]; 2, *Fuyii* [1969]; 3, *Harp and Jibson* [1995]; 4, *Hovius et al.* [1997]; 5, *Malamud and Turcotte* [1999]; 6, *Nielsen et al.* [1975]; 7, *Pelletier et al.* [1997]; 8, *Sugai et al* [1994].

[c]The last five rows correspond to catalogs of landslides on medium slope that provide only surface estimate measured by aerial photography. Accordingly, the range of volume used for these studies is not given in the fourth column. For these catalogs, volume exponents are derived from surface size distributions according to the *Hovius et al.* [1997] conversion rule, assuming that landslide length is proportional to thickness and width. It implies area$\sim$ volume$^{2/3}$. Then starting with $N(V) \sim V^{-b}$, $N(V)$ being the number of events with a volume larger than V, implies $N(A) \sim A^{-2b/3}$ for cumulative areas.

[31] As noted above, one study uses a continuous seismic monitoring to detect rockfall events and to size up rockfall volumes on a single, well-defined cliff [*Rousseau*, 1999]. This sampling method and the measurement technique provide a catalog that is not affected by the same biases as the data previously described. The volume distribution derived from Rousseau's catalog also follows a power law distribution (Table 2). First, this result supports the hypothesis that the power law derived from volumes estimated by field evaluations is not a measurement artifact. Second, it shows that a single cliff displays a power law volume distribution. It argues against the power law distribution to result from a geometrical effect, i.e., the power law does not result from an integration process over cliffs of different heights. Using the seismic monitoring technique, the exponent value of the power law is the largest reported value in the available catalogs for rockfalls on subvertical cliffs (Table 2). It may be due to the assumption made to derive the rockfall volume from the seismic amplitude. Seismological volume estimates are supposed to scale with the amplitude of seismic signals [*Rousseau*, 1999], but this relation may be incorrect. Assuming that seismic amplitude scales with the square root of the rockfall volume, as also proposed by K. Aki (personal communication, 2002), the exponent of rockfall volume distribution would be 0.5 instead of 1, in agreement with other studies reported on Table 2. Comparisons of both seismological signals and rockfall volumes are necessary to validate the relation between volumes and amplitudes of seismic signals.

[32] The power law distribution has also been reported for mixed landslides (Table 3 and references therein). From our study, which focus on the rockfall volumes that occurred on subvertical cliffs of stiff rock mass, we derive a b value that is significantly smaller than the average exponent value, 1.2 ± 0.3, estimated from studies that mixed different types of landslides (Table 3). The exponents are volume exponents or surface exponents that were converted to volume using the rule of *Hovius et al.* [1997] when exponent value for volume are not available (Table 3). We use this conversion rule on the same type of catalogs (Table 3) than the Hovius et al. study. This study hypothesizes that landslide length is proportional to thickness and width. Accordingly in absence of other tools and for the robustness of comparison between catalogs, we choose to use the rule of *Hovius et al.* [1997] (detailed in Table 3). For all the cases listed in Table 3, reported landslides occur either on less steep topography or involve softer unconsolidated material than rockfalls reported in Table 2.

4.2. Implication for Rockfall Hazard

[33] From the examples analyzed in the previous sections, the hypothesis that the volume distributions of natural rockfalls follow a power law distribution is accepted at a 90% confidence level. This distribution law provides the probability of occurrence of a given volume in a given time period on a given area and has been used for hazard assessment by *Hungr et al.* [1999] for rockfalls on man-made slopes. Using the Grenoble data set as a test example, we can derive the occurrence rate of a given volume range by using the power law,

$$N(V) = \frac{N_0}{T}\left(\frac{V}{V_0}\right)^{-b}, \tag{6}$$

$N(V)$ being the number of events per unit time with a volume larger than V for a catalog of duration T. N_0 is the number of events with a volume larger than V_0. For the Grenoble inventory, $V_0 = 40$ m^3, $N_0 = 55$, the catalog duration we analyzed is $T = 60$ years.

[34] The return period of a rockfall of volume larger than or equal to V is given by

$$t(V) = \frac{1}{N(V)}. \tag{7}$$

Using equations (6) and (7), we obtain a 10 years return period for a 10^4 m^3 event, or an average of four 10^5 m^3 events within a century. The largest historical event reported in the last thousand years in the Grenoble area is the 1248 Mount Granier rock avalanche of 5×10^8 m^3. From the power law distribution based on the 1935–1995 data, we derive a return period of 870 years for a Mount Granier size event. Therefore the largest observed event on a thousand-year period agrees with the return period for this volume. For this region the saturation volume for which the scaling

law could change is roughly $(h_{max})^3$, h_{max} being the maximum cliff height, with $(h_{max})^3 \sim 10^9$ m^3 for Grenoble cliffs. This value is a first-order estimate which includes the two levels of the Grenoble cliffs (Figure 1). Accordingly, the distribution must not be extrapolated to volumes larger than 10^9 m^3. Regarding the space domain, the presently limited number of data does not allow us to investigate spatial variations of rockfall occurrence rate. We can just provide the probability of occurrence for the whole studied area [*Vengeon et al.*, 2001].

4.3. Possible Models for Power Law Distributions of Rockfall Volumes

[35] There has not been yet any model which simulates specifically rockfall dynamics. One class of numerical models examines erosion; it can also apply to rockfall or landslide simulations [*Hergarten and Neugebauer*, 1998; *Densmore et al.*, 1998]. The second class of models includes generic models that can apply to a large range of phenomena that exhibit scale-invariant behavior, i.e., fragmentation and sand piles models.

4.3.1. Erosion-Type Model

[36] *Densmore et al.* [1998] proposed a numerical model that uses a slope stability criterion to simulate mechanics of hillslope failures. They obtain a power law distribution of volumes of mass movements. The exponent value of the simulated cumulative distribution varies as a function of the mechanical properties of the rock mass (cohesion and friction angle), from 1.2 for soft rock to 0.8 for hard rock. The authors suggest in their numerical simulation that a higher strength leads to steeper critical hill slope heights. Because in this model [*Densmore et al.*, 1998; *Champel et al.*, 2002] a higher strength corresponds to a steeper topography, simulations with stiff rock parameters may be related to rockfall circumstances on a subvertical cliff. Alternatively, we propose that other landslide types, which occurred on gentler slopes could be related to simulations with low strength materials that induce a larger exponent value for the power law distribution of volumes.

[37] For mixed landslide types, the observed b values (the exponents of the cumulative volume distributions), are in the range 0.7–1.3, with an average value $b = 1.2 \pm 0.3$ (Table 3). These values are significantly larger than those reported for rockfalls on subvertical cliffs. For rockfall settings (Table 2), i.e., stiff rock on subvertical cliffs characterized by a friction angle close to 35–45° [*Hoek and Brown*, 1980], the corresponding b values range from 0.2 to 1, with an average value of 0.5 ± 0.2. Therefore the models of [*Densmore et al.*, 1998; *Champel et al.*, 2002] qualitatively predict the observed changes in exponents between mixed landslide types that occurred on gentle slope topography (Table 3) and rockfalls on subvertical cliffs (Table 2). According to this model, the change in exponent values is driven by changes in the mechanical properties (e.g., internal friction angle or cohesion) of the involved rock mass. Stiff rocks, with a higher friction angle, generate steeper topographic slopes and lower exponent values than softer rocks.

4.3.2. Fragmentation Model

[38] From a generic point of view, the power law distribution observed for rockfall volumes (Table 2) is also similar to the fragment size distribution reported during fragmentation experiments [e.g., *Turcotte*, 1986, and references therein]. A power law distribution is admitted to characterize the distribution of fragments for a variety of rocks in laboratory experiments [e.g., *Turcotte*, 1986, and references therein]. Observed exponent values for cumulative volume distributions of fragments range from 0.5 to 1.2, with 0.8 as an average value. A generic model of fragmentation generates a power distribution of fragments, with a b exponent of the cumulative volume distribution defined by,

$$b = \frac{\log(8p)}{\log(8)}, \tag{8}$$

where p is the probability of a given cell of size l to break in 8 fragments of size l/2. This breaking rule is scale invariant; that is, each subcell whatever its size has the same probability p to break in 8 smaller cells [*Turcotte*, 1986]. Tuning of p values allows recovering observed exponent values for rock fragmentation with $b < 1$ for p ranging from 0 to 1. In this way, the power law distribution of rockfall volumes, with an exponent value ranging from 0.2 to 1 (Table 2), can be reproduced by this generic fragmentation model. Note that the observed exponents for rockfalls, 0.5 ± 0.2, are in the same range as those reported for fragmentation.

[39] It argues for the rockfall sizes to be possibly driven by the fragmentation process of the cliff, i.e., the preexisting discontinuity pattern. Accordingly, the rock mass fragment size should control the rockfall volume size, while neither cascade nor avalanche process should influence the rockfall volume distribution. This model can reproduce the observed distribution of rockfall volumes if the largest fragments are larger than the largest observed rockfall. Although the preexisting discontinuity pattern that controls the fragment size distribution is not extensively known for the studied cliffs, we observe that the number of rock blocks cut by discontinuities decreases rapidly when their size increases. It argues for possible large fragment sizes on our studied cliffs.

4.3.3. Sandpile-Type Model

[40] Another alternative to generate power law distributions is the conceptual sandpile model of *Bak et al.* [1987]. For rockfall dynamics, the scale-invariant rockfall distribution could arise solely from the dynamic of mechanical processes without requiring any preexisting scale-invariant heterogeneity. Cellular automaton models simulate avalanches on a sandpile. Three-dimensional numerical simulations yield an exponent value of 0.37 [*Bak et al.*, 1987; *Bak and Tang*, 1989], close to those we report for natural rockfalls. However this 3-D model generates avalanches which take place in the bulk of a volume. Accordingly, the mapping on the whole rock avalanches is difficult because most rockfalls occur on the surface of cliff. The model that is usually interpreted in terms of sand pile is the 2-D version of the model which yields a power law distribution with an exponent close to zero [*Bak et al.*, 1987; *Bak and Tang*, 1989]. This later exponent value is further away from the observed rockfall size distribution. However, a variety of cellular automaton models can account for a change in exponent value when modifying the interaction rules or the loading rules of the generic sand pile model from *Bak et al.*

Table 4. Possible Conceptual Models for Rockfall and Landslide Distribution

Generic Type	Ref[a]	Loading	Breaking Rules	*b* Value[b]	Application
Landslide model of rock erosion	2	tectonic uplift, gravity, fluvial cut	slope stability as function of friction and cohesion	0.8	rockfall
Landslide model of rock erosion	2	tectonic uplift, gravity, fluvial cut	slope stability as function of friction and cohesion	1.2	landslide
Landslide model of layered soil	3	tectonic uplift gravity, fluvial cut	slope gradient as function of layer thickness	0.70	landslide
Sandpile cellular-automata	1	additional sand grains	critical slope angle	~0, (2-D) ~0.4, (3-D)	landslide and rockfall
Fragmentation	4	no loading	fragmentation as a probability law (p)	<1, adjusted as $f(p)$	rockfall

[a]References are 1, *Bak et al.* [1987]; 2, *Densmore et al.* [1998]; 3, *Hergarten and Neugebauer* [1998]; 4, *Turcotte* [1986].
[b]All the exponent values are exponents of cumulative volume distributions.

[1987] [e.g., *Olami et al.*, 1992; *Amaral and Lauritsen*, 1997]. Therefore these models could explain the *b* value observed for the distribution of rockfall volumes. Without any other observational constrains on rockfall dynamics, we cannot decide which of the interactions rules or loading conditions of these different models are the more prone to capture the genuine rockfall dynamics.

[41] Contrary to the fragmentation model, the sandpile model simulates a power law distribution of volumes that emerges solely from the dynamics without any input of quenched heterogeneity [e.g., *Bak et al.*, 1987]. This model can be applied to any dynamic system characterized by a threshold dynamic, a stationary state, a slow exogenous driving when compared to the energy released, and a power law distribution of energy released. Within this context, the driven forces for a rockfall dynamical system are both the slow tectonic uplift rate, the fluvial down cutting and the constant gravity force. They have characteristic timescales, which are well separated from the time life of one single rockfall event. On such a basis, the dynamics of rockfall process share the same properties as the one proposed for earthquakes, i.e., a slow driving relatively to the relaxation process and a power distribution of relaxed energy [*Bak and Tang*, 1989; *Sornette and Sornette*, 1989; *Main*, 1996; *Grasso and Sornette*, 1998; *Vespignani and Zapperi*, 1998]. As suggested for landslides of unconsolidated material on moderate slope by *Hergarten and Neugebauer* [1998], it argues for rockfall dynamics to be another example of out of equilibrium, scale-free phenomena that could be generic to earth crust deformation processes.

[42] As a tentative mapping of each class of models on rockfall dynamics from subvertical cliffs and other landslide types respectively, we summarize the advantages and drawbacks of each model (Table 4). Possible applications of these models to reproduce landslide or rockfall cannot be sorted by using the exponent values of distribution. They come out from the specific hypothesis relevant to each model, i.e., erosion model, a sandpile cellular automaton, fragmentation. Erosion models that introduce realistic mechanical properties of the cliff in the generic sandpile model appear to capture the basic patterns of the landslide and rockfall distributions [e.g., *Densmore et al.*, 1998; *Hergarten and Neugebauer*, 1998]. If a fragmentation model is generically acceptable for rockfalls on subvertical cliffs, including simulated exponent values, it is rejected as a model for the soft unconsolidated material involved in other landslide types. Similarly, the soil erosion model of *Hergarten and Neugebauer* [1998] is well suited to simulate landslides of layered soft material, but the exponent value and the layered model assumption itself reject the possibility for this model to reproduce rockfall dynamics of subvertical cliffs. The erosion model of *Densmore et al.* [1998] is able to reproduce a change in exponent values that is observed when switching from events which originate on subvertical cliffs of stiff rock to event occurring on gentle slopes of softer materials [*Densmore et al.*, 1998; *Champel et al.*, 2002].

5. Conclusion

[43] We have analyzed three rockfall data sets on subvertical cliffs and we have shown that the rockfall volume distribution follows a power law distribution for volumes ranging from 10^2 to 10^{10} m^3, with the exponents *b* in the range [0.4–0.6] for the three catalogs. This exponent is also in agreement with previous studies of rockfalls along road cuts. We suggest two classes of models than can reproduce the power law distribution of rockfall volumes.

[44] First, the conceptual sandpile model of [*Bak et al.*, 1987; *Bak and Tang*, 1989] can reproduce the avalanche-like behavior of the rockfall activity. Accordingly the power law distribution of rockfall volumes is the avalanche like response to a slow loading rate, as driven by tectonic deformation and fluvial incision rates, when compared to the timescales of rock avalanches. This argues for the rockfall dynamics to be another class of out of equilibrium, scale-free phenomena as suggested for a large variety of earth crust deformation processes. In this context, the power law distribution of rockfall volumes would arise solely from the dynamic of the system and would not be affected by the preexisting heterogeneity pattern.

[45] Second, the observed power law distribution of rockfall volumes is similar to the one reported for both fragmentation experiments and fragmentation models. This argues for the in situ rock mass fragment sizes to possibly control the rockfall volumes. In this context, the rockfall volume distribution should be similar to the fragment size distribution, and neither cascade nor avalanche processes would influence the rockfall volume distribution.

[46] When comparing our observations of rockfalls on subvertical cliffs with different types of landslides, the exponent of the volume distribution is smaller for rockfalls than for landslides involving unconsolidated material occurring on less steep slopes. It argues for the rock mass properties, which constrain the topography slope in numer-

ical simulation [*Densmore et al.*, 1998; *Champel et al.*, 2002], to drive the change in exponent values for different landslide types and geomechanical settings.

[47] **Acknowledgments.** We gratefully thank R. Couture, J.P. Requillard and G. Wieczorek, who made the data available for the three inventories we used in this study, worldwide inventory, Grenoble area and Yosemite Valley, respectively. Unpublished detailed comments on their own landslides and rockfall studies by K. Aki, B. Champel, N. Hovius, D. Keefer, J. Pelletier, N. Rousseau, and C. Stark helped to clarify the final version of the paper. J.M. Vengeon is acknowledged for his fruitful discussions and R. Archuleta, A. McGarr, and G. Wieczorek are thanked for their comments on an initial version of the manuscript. Detailed reviews by A. Densmore and S. Hergarten improved the quality of the manuscript.

References

Aki, K., Maximum likelihood estimate of b in the formula $\log N = a - bM$ and its confidence limits, *Bull. Earthquake Res. Inst. Univ. Tokyo*, *43*, 237–239, 1965.

Amaral, L. A. N., and K. B. Lauritsen, Universality classes for rice-pile models, *Phys. Rev. E*, *56*, 231–234, 1997.

Bak, P., and C. Tang, Earthquakes as a self-organized critical phenomenon, *J. Geophys. Res.*, *94*, 15,635–15,637, 1989.

Bak, P., C. Tang, and K. Wiesenfeld, Self-organized criticality, *Phys. Rev. A*, *38*, 364–374, 1987.

Blodgett, T. A., B. L. Isacks, E. J. Fielding, J. G. Masek, and A. S. Warner, Erosion attributed to landslides in the Cordillera Real, Bolivia, *Eos Trans. AGU*, *77*(17), Spring Meet. Suppl., S261, 1996.

Champel, B., P. van der Beek, J.-L. Mugnier, and P. Leturmy, Growth and lateral propagation of fault-related folds in the Siwaliks of western Nepal: Rates, mechanisms, and geomorphic signature, *J. Geophys. Res.*, *107*(B6), 2111, doi:10.1029/2001JB000578, 2002.

Couture, R., Contribution aux aspects mécaniques et physiques des écroulements rocheux: Génie géologique, Ph.D. thesis, pp. 56–65, Univ. of Laval, Saint-Foy, Quebec, 1998.

Densmore, A., M. Ellis, and R. Anderson, Landsliding and the evolution of normal-fault-bounded mountains, *J. Geophys. Res.*, *103*, 15,203–15,219, 1998.

Dixon, T. H., M. Miller, F. Farina, H. Wang, and D. Johnson, Present-day motion of the Sierra Nevada block and some tectonic implications for the Basin and Range province, North American Cordillera, *Tectonics*, *19*, 1–24, 2000.

Fréchet, J., Sismicité du Sud-Est de la France et une nouvelle méthode de zonage sismique, Thèse 3ème cycle, 159 pp., Univ. de Grenoble, Grenoble, France, 1978.

Fuyii, Y., Frequency distribution of the landslides caused by heavy rain-fall, *J. Seismol. Soc. Jpn.*, *22*, 244–247, 1969.

Gardner, J., Rockfall: A geomorphic process in high mountain terrain, *Albertan Geogr.*, *6*, 15–20, 1970.

Goguel, J., and A. Pachoud, Géologie et dynamique de l'écroulement du Mont Granier, dans le massif de la Chartreuse, en novembre 1248, *Bull. BRGM*, *III*(1), 29–38, 1972.

Grasso, J. R., and D. Sornette, Testing self-organized criticality by induced seismicity, *J. Geophys. Res.*, *103*, 29,965–29,987, 1998.

Grasso, J.-R., F. Guyoton, J. Fréchet, and J. F. Gamond, Triggered earthquakes as stress gauge: Implication for the upper crust behavior in the Grenoble area France, *Pure Appl. Geophys.*, *139*, 579–605, 1992.

Guillot, P., and R. Duband, La méthode du GRADEX pour le calcul de la probabilité de crues partir des pluies, *IASH Publ.*, 84, 1967.

Gutenberg, B., and C. F. Richter, *Seismicity of the Earth and Associated Phenomena*, Princeton Univ. Press, Princeton, N. J., 1949.

Harp, E. L., and R. L. Jibson, Inventory of landslide triggered by the 1994 Northridge California earthquake, *U.S. Geol. Surv. Open File Rep.*, 95–213, 1995.

Hergarten, S., and J. Neugebauer, Self-organized criticality in a landslide model, *Geophys. Res. Lett.*, *25*, 801–804, 1998.

Hoek, E., and E. T. Brown, *Underground Excavations in Rock*, Inst. of Min. and Metall., London, 1980.

Hovius, N., C. P. Stark, and P. A. Allen, Sediment flux from a mountain belt derived by landslide mapping, *Geology*, *25*, 231–234, 1997.

Huber, N. K., The geologic story of Yosemite National Park, *U.S. Geol. Surv. Bull.*, *1595*, 59, 1987.

Hungr, O., S. G. Evans, and J. Hazzard, Magnitude and frequency of rock falls along the main transportation corridors of southwestern British Columbia, *Can. Geotech. J.*, *36*, 224–238, 1999.

Keefer, D. K., Rock avalanches caused by earthquakes: Source characteristics, *Science*, *223*, 1288–1290, 1984.

Keefer, D. K., Earthquake-induced landslides and their effects on alluvial fans, *J. Sediment. Res.*, *69*(1), 84–104, 1999.

Main, I., Statistical physics: Seismographs and seismic hazard, *Rev. Geophys.*, *34*, 433–462, 1996.

Malamud, B. D., and D. L. Turcotte, Self-organized criticality applied to natural hazards, *Nat. Hazards*, *20*, 93–116, 1999.

Martinod, J., F. Jouanne, J. Taverna, G. Menard, J. F. Gamond, X. Darmantrail, J. C. Notter, and C. Basile, Present-day deformation of the Dauphine (SE France) Alpine and Subalpine massifs, *Geophys. J. Int.*, *127*, 189–200, 1996.

Nielsen, T. H., J. A. Bartow Jr., V. A. Frizell, and J. D. Sims, Preliminary photointerpretation maps of landslides and other superficial deposits of 567 1/2-minutes quadrangle in the southeastern San Francisco Bay region, Alameda, Contra costa and Santa Clara countries, California, *U.S. Geol Surv. Open File Rep., 75–0277*, 1975.

Noever, D. A., Himalayan sandpiles, *Phys. Rev. E*, *47*, 724–725, 1993.

Olami, Z., H. J. S. Feder, and K. Christensen, Self-Organized Criticality in a continuous non-conservative cellular automaton modeling earthquakes, *Phys. Rev. Lett.*, *68*, 1244–1247, 1992.

Pelletier, J. D., B. D. Malamud, T. A. Blodgett, and D. L. Turcotte, Scale invariance of soil moisture variability and its implications for the frequency size distribution of landslides, *Eng. Geol.*, *48*, 255–268, 1997.

Pickering, G., J. M. Bull, and D. J. Sanderson, Sampling power law distribution, *Tectonophysics*, *48*, 1–3, 1995.

Press, W. H., S. A. Teukolsky, W. T. Vettering, and B. P. Flannery, *Numerical Recipes in C*, 994 pp., Cambridge Univ. Press, New York, 1992.

Rousseau, N., Study of seismic signals associated with rockfalls at 2 sites on the Reunion Island (Mahavel Cascade and Souffriére cavity), Ph.D. thesis, Inst. de Phys. du Globe de Paris, Paris, 1999.

Service de Restauration des Terrains en Montagne de l'Isére (RTM), Inventaire des mouvements rocheux, Secteur de l'Y grenoblois, Grenoble, France, 1996.

Sornette, A., and D. Sornette, Self-organized criticality and earthquakes, *Europhys. Lett.*, *9*, 197–202, 1989.

Stark, C. P., and N. Hovius, The characterization of landslides size distributions, *Geophys. Res. Lett.*, *28*, 1091–1094, 2001.

Sugai, T., H. Ohmori, and M. Hirano, Rock control on magnitude-frequency distribution of landslides, *Trans. Jpn. Geomorph. Union*, *15*, 233–351, 1994.

Taylor, J. R., *An Introduction to Error Analysis*, 2nd ed., 327 pp., Univ. Sci. Books, Sausalito, Calif., 1997.

Turcotte, D., Fractals and fragmentation, *J. Geophys. Res.*, *91*, 1921–1926, 1986.

U.S. Water Resources Council, Guidelines for determining flood flow frequency, *Bull. 17B*, 182 pp., Hydrol. Subcomm., Off. of Water Data Coord., U.S. Geol. Surv., Reston, Va., 1982.

Varnes, D. J., Slope movements: Types and processes. In: Landslide analysis and control, *Spec. Rep. 176*, pp. 11–33, Transp. Res. Board, Natl. Acad. of Sci., Washington, D. C., 1978.

Vengeon, J. M., D. Hantz, and C. Dussauge, Predictabilité des éboulements rocheux: Approche probabiliste par combinaison d'études historiques et géomécaniques, *Rev. Fr. Géotech.*, *95–96*, 143–153, 2001.

Vespignani, A., and S. Zapperi, How self-organized criticality works: A unified mean field picture, *Phys. Rev. E*, *57*, 6345–6362, 1998.

Wesnousky, S., C. Scholz, K. Shimazaki, and T. Matsuda, Earthquake frequency distribution and the mechanics of faulting, *J. Geophys. Res.*, *88*, 9331–9340, 1983.

Wesnousky, S., C. Scholz, K. Shimazaki, and T. Matsuda, Integration of geological and seismological data for the analysis of seismic hazard: A case study of Japan, *Bull. Seismol. Soc. Am.*, *74*, 687–708, 1984.

Wieczorek, G. F., J. B. Snyder, C. S. Alger, and K. A. Isaacson, Yosemite historical rockfall inventory, *U.S Geol. Surv. Open File Rep., 92–387*, 38 pp., 1992.

Wieczorek, G. F., S. P. Nishenko, and D. J. Varnes, Analysis of rock falls in the Yosemite Valley, California, *Proc. U.S. Symp. Rock Mech.*, *35th*, 85–89, 1995.

C. Dussauge, Laboratoire Interdisciplinaire de Géologie et de Mécanique, Université Joseph Fourier, BP 53X, 38041 Grenoble Cedex, France. (carine.dussauge@ujf-grenoble.fr)

J.-R. Grasso, Institute of Geophysics and Planetary Physics, 3845 Slichter Hall, University of California, Los Angeles, CA 90095-1567, USA. (grasso@moho.ess.ucla.edu)

A. Helmstetter, Laboratoire de Géophysique Interne et Tectonophysique, Observatoire de Grenoble, Université Joseph Fourier, BP 53X, 38041 Grenoble Cedex, France. (ahelmste@obs.ujf-grenoble.fr)